



UNIVERSITÀ DI PISA



# Commissioning of the Mu2e tracker DAQ, planning for the Vertical Slice Test and pre-pattern recognition studies

Candidate:

Sara Gamba

Supervisors:

Pavel Murat (FNAL)

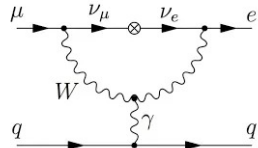
Simone Donati (Unipi, INFN Pisa)

October 21<sup>st</sup> 2024

# Charged Lepton Flavour Violation

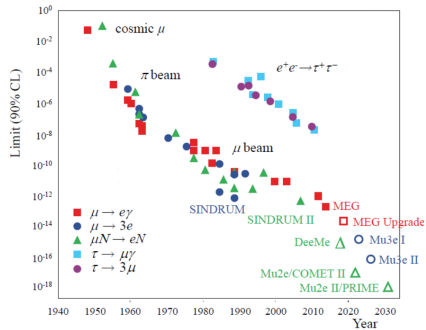
- The **Standard Model** (SM) does not predict lepton flavour violation;
- The discovery of **neutrino oscillations** proves that lepton interactions are non-diagonal in flavour;
- The SM fails to explain phenomena like neutrino masses and the consequent flavour oscillations;
- The branching ratios of **CLFV** processes, including neutrino oscillations, are suppressed by factors proportional to  $(\Delta m_\nu^2)^2/M_W^4$  and expected to be less than  $\mathcal{O}(10^{-50})$ ;
- This value is far beyond current experimental capabilities.

QUARKS		
mass $=2.2 \text{ MeV}/c^2$	$\frac{2}{3}$	$\frac{2}{3}$
charge $\frac{2}{3}$	$\frac{1}{2}$	$\frac{1}{2}$
spin $\frac{1}{2}$	u	c
	up	charm
mass $=4.7 \text{ MeV}/c^2$	$-1$	$-1$
charge $-1/3$	$\frac{1}{2}$	$\frac{1}{2}$
spin $\frac{1}{2}$	d	s
	down	strange
mass $=173.1 \text{ GeV}/c^2$	$\frac{2}{3}$	$\frac{2}{3}$
charge $\frac{2}{3}$	$\frac{1}{2}$	$\frac{1}{2}$
spin $\frac{1}{2}$	t	b
	top	bottom
LEPTONS		
mass $=0.511 \text{ MeV}/c^2$	$-1$	$-1$
charge $-1$	$\frac{1}{2}$	$\frac{1}{2}$
spin $\frac{1}{2}$	e	$\mu$
	electron	muon
mass $=1.7768 \text{ GeV}/c^2$	$-1$	$-1$
charge $-1$	$\frac{1}{2}$	$\frac{1}{2}$
spin $\frac{1}{2}$	$\tau$	tau
mass $<1.0 \text{ eV}/c^2$	$0$	$0$
charge $0$	$\frac{1}{2}$	$\frac{1}{2}$
spin $\frac{1}{2}$	$\nu_e$	$\nu_\mu$
mass $<0.17 \text{ MeV}/c^2$	$0$	$0$
charge $0$	$\frac{1}{2}$	$\frac{1}{2}$
spin $\frac{1}{2}$	$\nu_\tau$	$\nu_\tau$
mass $<18.2 \text{ MeV}/c^2$	$0$	$0$
charge $0$	$\frac{1}{2}$	$\frac{1}{2}$
spin $\frac{1}{2}$		
mass $<18.2 \text{ MeV}/c^2$	$0$	$0$
charge $0$	$\frac{1}{2}$	$\frac{1}{2}$
spin $\frac{1}{2}$		



# Search for CLFV

- ▶ New Physics (NP) models predict much higher rates of CLFV;
- ▶ Observing CLFV would provide unambiguous evidence of physics beyond the SM;
- ▶ CLFV channels involving muons:  
 $\mu^+ \rightarrow e^+ \gamma$ ,  $\mu^- N \rightarrow e^- N$  and  
 $\mu^+ \rightarrow e^+ e^+ e^-$ ;
- ▶  $\mu^- N \rightarrow e^- N$  channel:
  - Higher momentum signal and better separation from the background;
  - Benefits from high intensity beam;
  - Better sensitivity to CLFV in a large range of NP scenarios.
- ▶ Current best limit on  $\mu^- N \rightarrow e^- N$  by SINDRUM II:  $R_{\mu e} < 7 \times 10^{-13}$  (90% CL).



# The Mu2e experiment

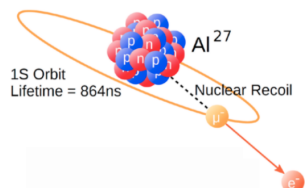
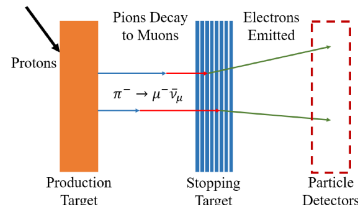
- ▶ Search for neutrinoless, coherent conversion  $\mu^- N \rightarrow e^- N$  in the field of an Al nucleus, by measuring:

$$R_{\mu e} = \frac{\mu^- + N(Z, A) \rightarrow e^- + N(Z, A)}{\mu^- + N(Z, A) \rightarrow \nu_\mu + N(Z - 1, A)}$$

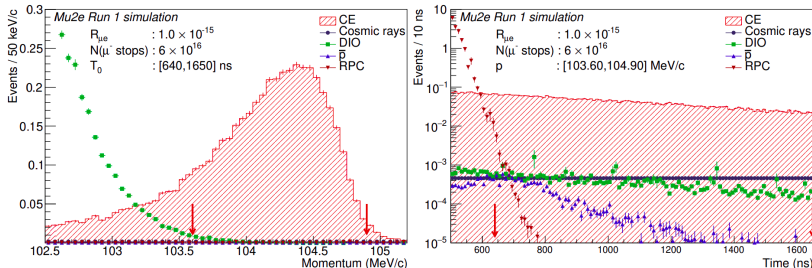
- ▶ Mu2e goal is to improve SINDRUM II limit by 4 orders of magnitude;
- ▶ The signal is a monochromatic conversion electron (CE) with energy:

$$E_{CE} = m_\mu - E_{recoil} - E_{bind} = 104.97 \text{ MeV}$$

where  $m_\mu$  is the muon mass,  $E_{recoil}$  the target nucleus recoil energy and  $E_{bind}$  the muonic atom  $1s$  state binding energy.

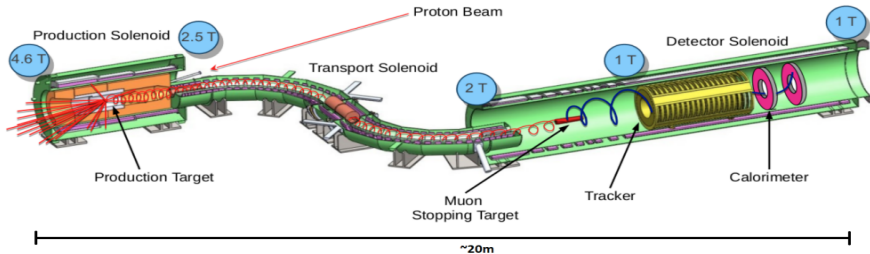


# Background sources



- ▶ **Cosmics** → veto enclosing the detector ( $\approx 0.046$  evs/RunI);
- ▶ **Intrinsic** → 1 MeV/c momentum resolution:
  - Decay In Orbit  $\mu^- N \rightarrow e^- \bar{\nu}_e \nu_\mu N$  ( $\approx 0.038$  evs/RunI);
  - Radiative Muon Capture  $\mu^- N \rightarrow \gamma \nu_\mu N'^*$  ( $< 0.0024$  evs/RunI).
- ▶ **Delayed processes from  $\bar{p} \rightarrow$**  absorbers in the TS ( $\approx 0.010$  evs/RunI);
- ▶ **Prompt processes** → pulsed beam + delayed live window:
  - Radiative Pion Capture  $\pi^- N \rightarrow \gamma N'^*$  ( $\approx 0.010$  evs/RunI);
  - $\pi$  and  $\mu$  Decay In Flight ( $< 2 \times 10^{-3}$  evs/RunI);
  - Beam electrons ( $< 1 \times 10^{-3}$  evs/RunI).

# The Mu2e experimental setup



## ► Production Solenoid:

- 8 GeV pulsed proton beam interacts with the W target and mostly  $\pi$ s are produced;
- graded field for backward collection.

## ► Transport Solenoid:

- it allows for  $\pi$  decay and  $\mu$  transport;
- S-shape for charged particle selection;
- it selects muons with  $p \lesssim 100$  MeV/c;
- rotating collimator COL3 selects  $\mu^-$  or  $\mu^+$  beam.

## ► Detector Solenoid: Stopping Target, $p$ absorber and detectors.

# The electromagnetic calorimeter

Calorimeter is vital for:

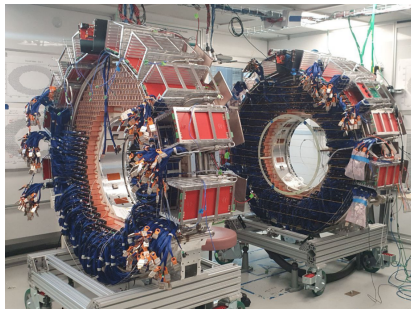
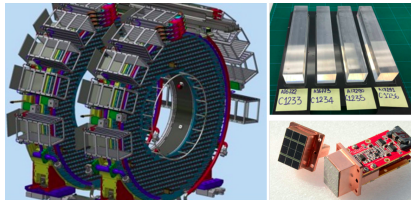
- ▶ **PID ( $E/p$ );**
- ▶ Seed for **track reconstruction**;
- ▶ Fast online **trigger filter**.

Design:

- ▶ 2 hollow disks of crystals, 70 cm apart;
- ▶  $2 \times 674$  CsI crystals per disk, each coupled to 2 SiPMs.

Performance:

- ▶  $\sigma_E/E \sim 10\%$ ;
- ▶  $\sigma_{xy} \sim 6$  mm;
- ▶  $\Delta t < 500$  ps.



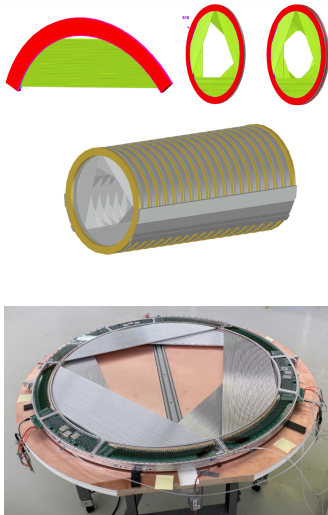
# The straw tracker

## Purpose:

- ▶ momentum measurement with  $\Delta p < 300 \text{ keV}/c \text{ FWHM} + 950 \text{ keV}/c$  energy losses (ST and proton absorber).

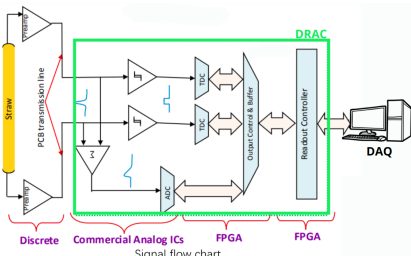
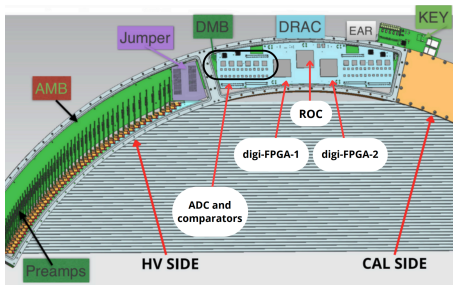
## Design:

- ▶ 3 m downstream of the ST ( $B \sim 1 \text{ T}$ );
- ▶ hollow geometry (low  $p_T$  particles);
- ▶ 3 m long tracker in vacuum;
- ▶ 96 straws per panel, 6 panels per plane, 2 planes per station;
- ▶ 18 tracking stations: 216 panels;
- ▶ 5 mm diameter and 40-110 cm long straws filled with a 80%:20% Ar:CO<sub>2</sub> mixture at a pressure of 1 atm.



# The tracker readout and DAQ

- ▶ Signal is readout from both ends by preamps;
- ▶ Analog signals are sent to the DRAC and processed by 2 TDCs and one ADC;
- ▶ The 2 digi-FPGA create one data packet for each hit with **two hit times** and **one waveform**;
- ▶ Data packets sent to ROC;
- ▶ ROC collects, buffers and transfers data from digi-FPGAs to DTC installed on DAQ computers;
- ▶ DTC sends data request to the ROC and sends data packet to the Event Builder.



# My Thesis

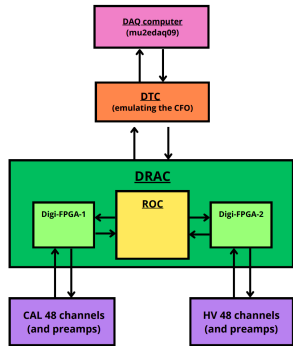
- ▶ Mu2e is starting detector **commissioning** and **calibration**;
- ▶ My work consists of a **comprehensive study of the Mu2e tracker**:
  - **Vertical Slice Test (VST)**. The entire testing chain, from the straws to the readout, to processed data on disk:
    - ▶ initial tracker **DAQ** and **FEE** testing.
  - First steps towards the tracker timing **calibration** with **cosmics**:
    - ▶ development of a **cosmic track reconstruction** procedure.
  - **Mu2e Offline**. Pre-pattern recognition studies:
    - ▶ estimated data volume for Mu2e data-taking is **>7 PB/year**;
    - ▶ the **primary source** of hits in the Mu2e tracker will be  $\delta$ -electrons;
    - ▶ important to identify those hits without losing **CE efficiency**.

# Outline

- ▶ Commissioning of the tracker DAQ and FEE:
  - validation of ROC readout;
  - study of preamplifiers performance.
- ▶ First steps towards the station calibration;
- ▶ Pre-pattern recognition studies;
- ▶ Conclusions.

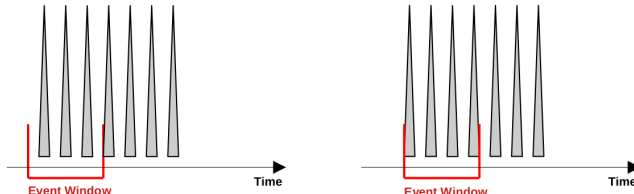
# Description of test stand setup

- ▶ ROC readout validation;
- ▶ TS1 tracker test stand: one ROC (one tracker panel-96 channels), one DTC connected to the DAQ computer;
- ▶ Two different ROC data readout modes:
  - MODE 1: emulated data readout mode;
  - MODE 2: digi-FPGA readout mode.
- ▶ digi-FPGAs pulsed by their **internal pulser** at  $f_{gen} = 250 \text{ kHz}$  or  $60 \text{ kHz}$ ;
- ▶ **Event Window ( $T_{EW}$ )**: the time interval between two proton pulses, varied between  $700 \text{ ns}$  to  $50 \mu\text{s}$ ;
- ▶ The ROC firmware has an internal **hit buffer** which stores up to **255 hits**.



# Logic of data taking

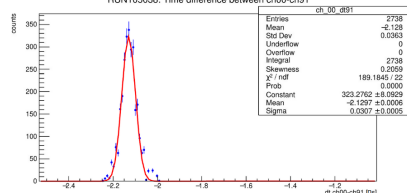
- ▶ Depending on  $T_{gen} = 1/f_{gen}$  and  $T_{EW}$ , the data taking can proceed in two different modes:
  - $N_{gen} \geq 255$ :  $N_{readout} = 255$  (**overflow mode**);
  - $N_{gen} < 255$ :  $N_{readout} < 255$  (**underflow mode**);
- ▶ Each FPGA has its own generator and pulses from different generators are offset ( $\in [0, T_{gen}]$ ) with respect to each other;
- ▶ Offsets between channels (same digi-FPGA) are about few ns and can be measured;
- ▶ Timing of generator pulses uncorrelated with the beginning of the EW  
→ different number of hits in an EW;
- ▶ Channel readout sequence is fixed.



# Monte Carlo simulation

- ROC readout logic emulated with a bit-level C++ simulation;
- Simulated parameters:
  - number of hits in each channel;
  - number of readout hits per event.
- digi-FPGAs and channel to channel offsets considered.

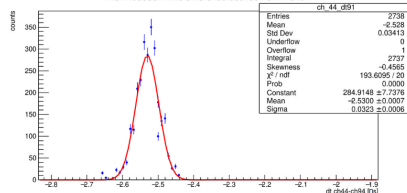
RUN105038: Time difference between ch00-ch91



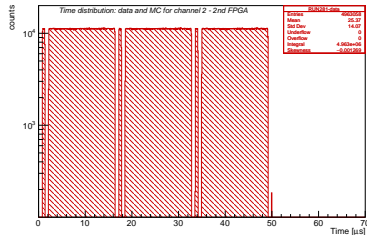
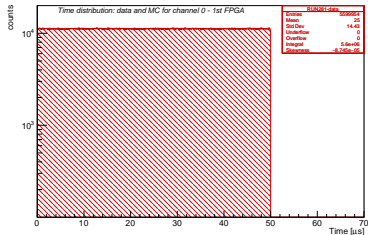
## Steps of the simulation:

- EW starts at  $t = 0$  s;
- The 1st pulse is generated  $T_0 \in [0, T_{gen}]$ ;
- Next pulses:  $T_i = T_{i-1} + T_{gen}$ , until  $T_i > T_{EW}$ ;
- Pulses are generated in each channel following the readout sequence;
- The procedure *continues* until all hits have been *readout*, or  $N_{hits} > 255$ .

RUN105038: Time difference between ch44-ch94



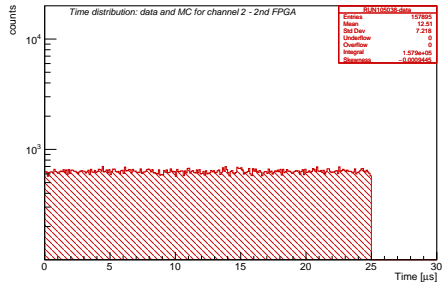
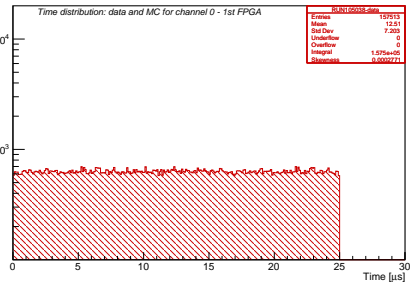
# Hit timing distribution: overflow mode



- ▶  $T_{EW} = 50 \mu\text{s}$  and  $f_{gen} = 60 \text{ kHz}$ ;
- ▶ The distribution of the hit time for channel 0 of digi-FPGA-1 (Left) and channel 2 of digi-FPGA-2 (Right);
- ▶ Different behaviour for different channels in different FPGAs: Left distribution is uniform, Right one is non-trivial;
- ▶ Apparently there are interruptions of channel 2 in the second FPGA;
- ▶ This behaviour can be explained with the *occupancy* plot.

# Hit timing distribution: regular mode

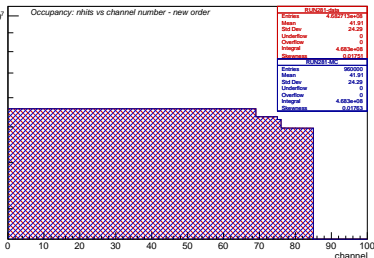
counts



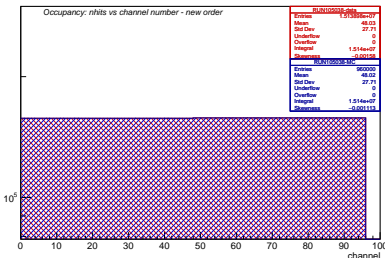
- ▶  $T_{EW} = 25 \mu\text{s}$  and  $f_{gen} = 60 \text{ kHz}$ ;
- ▶ The distribution of the hit time for channel 0 of digi-FPGA-1 (Left) and channel 2 of digi-FPGA-2 (Right);
- ▶ Same behaviour for different channels in different FPGAs;
- ▶ No interruptions of channel 2 in the second FPGA.

# Occupancy

counts

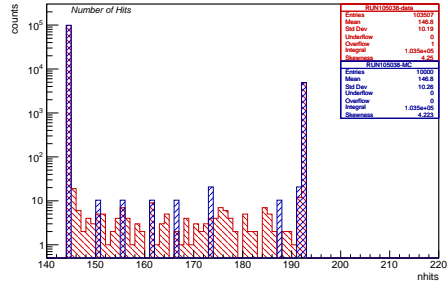
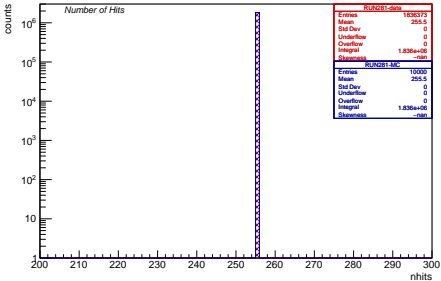


counts



- ▶ Occupancy plot: number of hits versus channel number (data red, MC blue);
- ▶ The bin ordering corresponds to the channel readout ordering;
- ▶ Overflow mode (Left):
  - channels 0-68: 48 digi-FPGA-1 channels with 4 hits (192 hits) and 21 digi-FPGA-2 channels with 3 hits (63 hits);
  - channels 0-75: 48 digi-FPGA-1 channels with 3 hits (144 hits) and 27 digi-FPGA-2 channels with 4 hits (108 hits) and 1 with 3 hits (111 hits);
  - channels 0-85: 48 digi-FPGA-1 channels with 3 hits (144 hits) and 37 digi-FPGA-2 channels with 3 hits (111 hits).
- ▶ Regular mode (Right): all channels with same occupancy.

# Number of hits



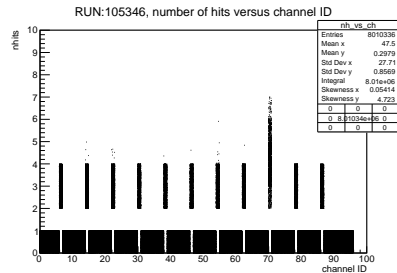
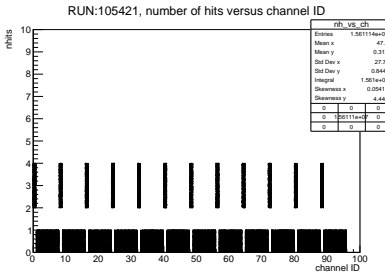
- ▶ Overflow mode (Left): distribution of number of hits peaked in 255;
- ▶ Regular mode (Right): the number of hits distribution depends on the relative offset of the EW with respect to the digi-FPGA pulsers and it varies from 144 to 192;
- ▶ Agreement between MC and data at a level of  $10^{-3}$ .

# Outline

- ▶ Commissioning of the tracker DAQ and FEE:
  - validation of ROC readout;
  - study of preamplifiers performance.
- ▶ First steps towards the station calibration;
- ▶ Pre-pattern recognition studies;
- ▶ Conclusions.

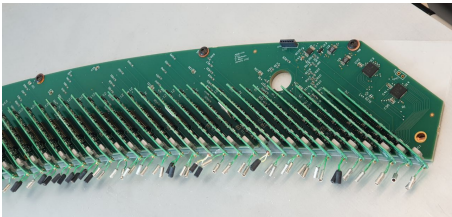
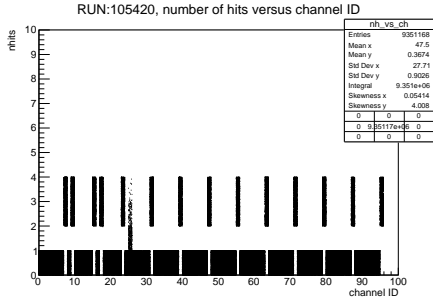
# Test 1: channel occupancy

- ▶ Same test stand: 1 or 2 ROCs and one DTC + CAL side preamps;
- ▶ digi-FPGA generates calibration pulses (every 8th channel across 12 RUNs);
- ▶ Looking for cross talks, non-uniform occupancy, dead channels;
- ▶ The frequency was set to 50 kHz and  $T_{EW} = 50 \mu\text{s}$ , 2 or 3 hits per channel.



- ▶ (Left): regular occupancy;
- ▶ (Right): 94th channel dead (preamp substituted) and  $N_{hits} > 3$  in some channels → waveforms shape study in Test 2.

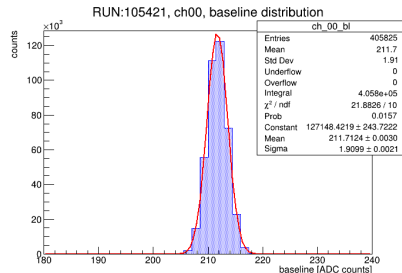
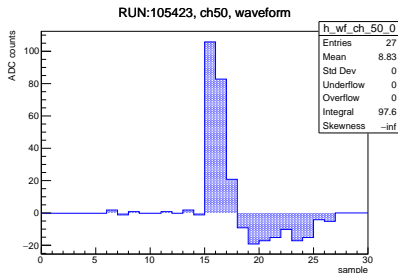
# Test 1: channel occupancy



- ▶ (Left): occupancy plot with cross talks in first odd channels and only asymmetric (e.g.  $3 \rightarrow 5$ , not seen  $3 \rightarrow 1$ );
- ▶ (Right): preamp boards are mounted vertically and odd channels are those on the PCB board;
- ▶ The distance between the first channels is slightly lower;
- ▶ The solution to these cross talks is still object of study.

## Test 2: analysis of readout waveforms shape

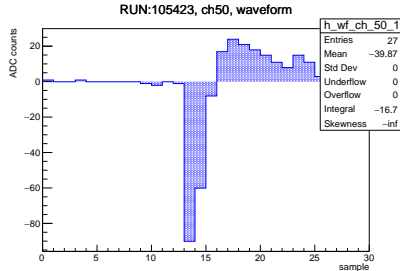
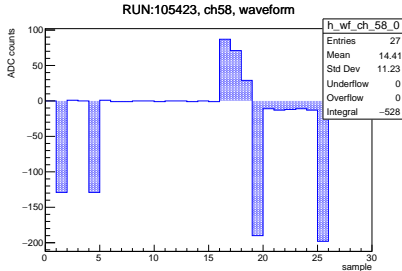
- ▶ Checking signal uniformity among channels within the same ROC or across multiple ROCs, and among different events;
- ▶ 40 MHz ADC (25 ns sample width) and pulser frequency set to 50 kHz.



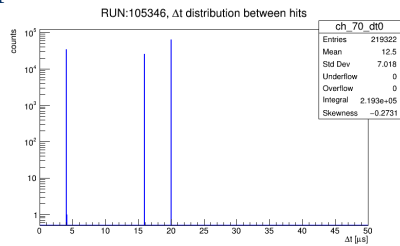
- ▶ (Left): regular waveform;
- ▶ Flat distribution in the first 10 samples (baseline), high positive charge peak with a sharp leading edge, negative tail;
- ▶ (Right): fitted baseline distribution, with mean at 210 ADC counts and  $\text{FWHM} = 2\sqrt{2\ln 2}\sigma \sim 4.5$  ADC counts.

# Test 2: analysis of readout waveforms shape

- Different baseline values indicating noise, dips, inverted waveforms.

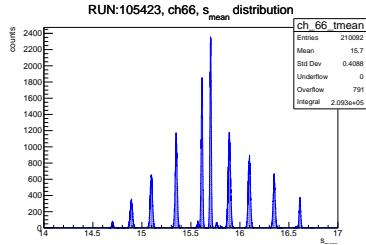
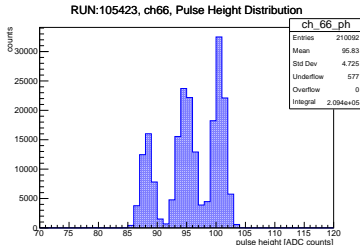


- (Left): dips of specific depths (64, 128 or 192) → ADC 6th or 7th bits;
- Problematic samples identified and excluded from the baseline estimate;
- (Right): inverted waveform →  $\Delta t$  distribution peaked in 16  $\mu s$  (regular) and 4  $\mu s$  (inverted). Trigger on trailing edge of 4  $\mu s$  long input pulses.

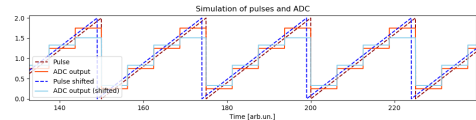


# Test 2: analysis of readout waveforms shape

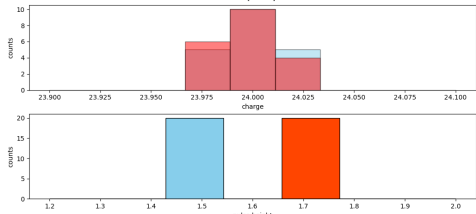
- (Left): pulse height (PH) (charge) distribution with 2/3 peaks.



- (Top Right):  $s_{\text{mean}} = \frac{\sum_i \text{sample}_i \cdot q_i}{\sum_i q_i}$  distribution, correlated with PH (charge) peaks;

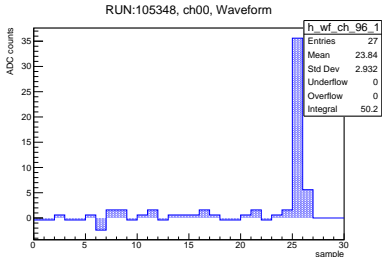
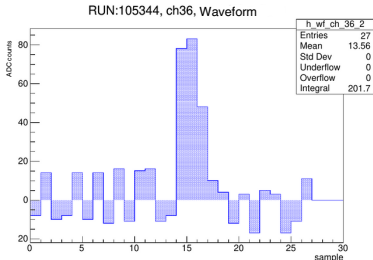


- (Bottom Right): simulation of the charge and PH distribution behaviour;

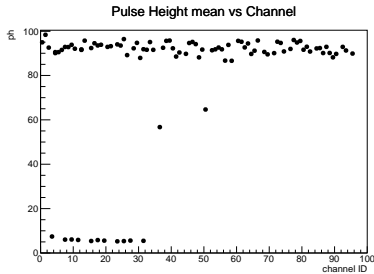
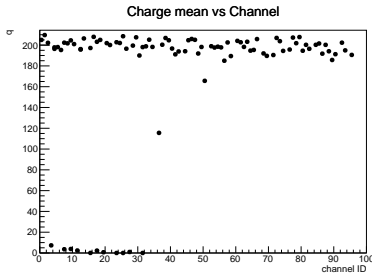


# Test 2: analysis of readout waveforms shape

- ▶ Charge distribution used to check noisy channels (Left) and glitches (Right).



- ▶ Check of the response uniformity across channels.



# Outline

- ▶ Commissioning of the tracker DAQ and FEE:
  - validation of ROC readout;
  - study of preamplifiers performance.
- ▶ First steps towards the station calibration;
- ▶ Pre-pattern recognition studies;
- ▶ Conclusions.

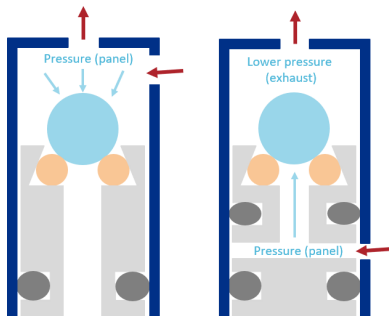
# First steps towards the station calibration

- ▶ **Calibration goal:** straw longitudinal position resolution  $\lesssim 4$  cm;
- ▶ TDCs measure arrival times  $t_1$  and  $t_2$ ;
- ▶  $v$ : signal propagation velocity;
- ▶  $x_{\text{track}}$ : reconstructed track on wire;
- ▶ **Calibration:**  $v$  from  $\Delta t_{12}$  (TDCs) correlated with  $x_{\text{track}}$  (**unbiased**);
- ▶  $x_{\text{track}}$  determined by straw "yes or no" information → **station geometry**.
- ▶ First calibration with **cosmics**;
- ▶ *Horizontal* → unbiased reconstruction;
- ▶ **Operational constraints:** gas system, space, fragility. Designed to be operated **vertically**;
- ▶ **Simulation with vertical station to assess biases and feasibility.**

$$t_1 = t_0 + \frac{x_{\text{track}}}{v} + t_d + d_1$$

$$t_2 = t_0 + \frac{L - x_{\text{track}}}{v} + t_d + d_2$$

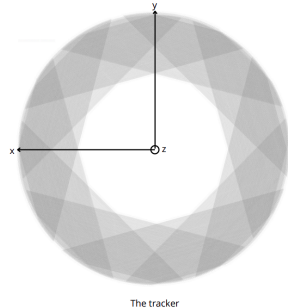
$$\Delta t_{12} = \frac{2x_{\text{track}} - L}{v} + (d_1 - d_2)$$



# Monte Carlo muon selection and reconstruction

## ► Cosmics as calibration source:

- standard detector operations;
- flux is  $\sim 1 \text{ cm}^{-2}\text{min}^{-1}$  (for horizontal detectors) and  $E_{mean} \sim \text{GeV}$ ;
- MIP;
- $v_\mu \sim c \rightarrow$  align channel offsets.



## ► Straw information:

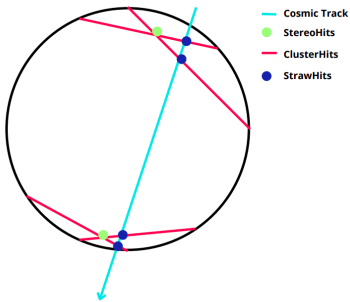
- the direction ( $D_{x,i}, D_{y,i}$ );
- the midpoint ( $M_{x,i}, M_{y,i}$ );
- the  $z_i$  coordinate.

## ► Selection:

- Hits in **one vertical station**;
- **Straight line in 3D**:  $\geq 4$  hits at different  $z \rightarrow nhits_{face_i} \geq 1$ ;
- **Resolution**:  $nhits_{panel_i} \leq 3$ .

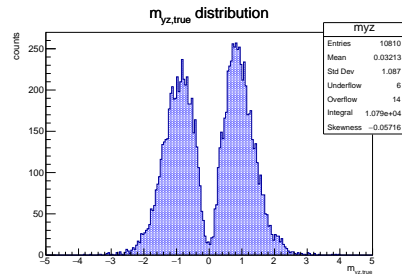
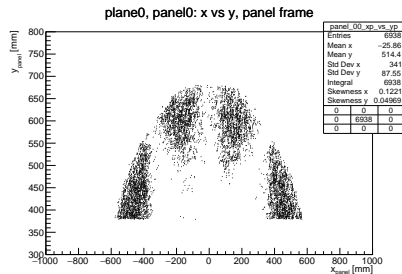
## ► Reconstruction:

- $StrawHits \rightarrow 1 ClusterHit$  (face);
- $2 ClusterHits \rightarrow StereoHit$  (plane);
- $2 StereoHits \rightarrow$  reconstructed track.



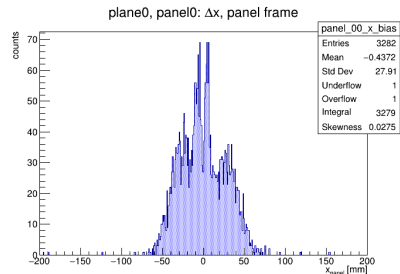
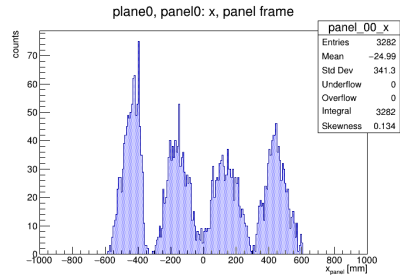
# Panel illumination pattern and muon directions

- Precise calibration: uniformly distributed hits across the panel;
- (Top): muon selections bring to **non uniform** and spotty panel illumination;
- 4/4 overlap areas limited to **panel edges**;
- Time walk effects**;
- Selection of **specific muon directions**;
- (Bottom):  $m_{yz} = \Delta y / \Delta z$  distribution;
- No particles with  $m_{yz} \sim 0$  (horizontal) and  $m_{yz} \rightarrow \infty$  (vertical);
- Mostly with  $|m_{yz}| \sim 1$  (**45° angle**);
- Muon **rate** scaled by  $1 / \cos^2 \theta \sim 1/2$  (45° flux) and  $1/\sqrt{2}$  (cosmics striking at 45°).



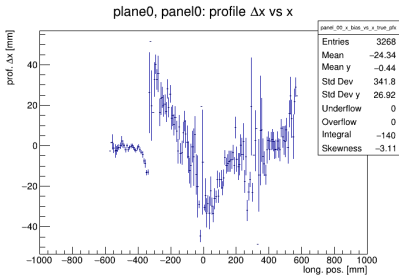
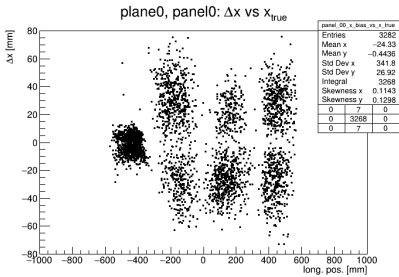
# Longitudinal position reconstruction

- (Top): longitudinal reconstructed position  $x_{track}$  (panel frame);
- $x_{track}$ : intersection of the reconstructed track with the mean  $z_i$  of the panel;
- **Bumps**  $\rightarrow$  4/4 requirement consequence;
- Different bumps  $\rightarrow$  different straws;
- (Bottom): longitudinal reconstructed position **bias** (panel frame);
- $\Delta x = x_{track} - x_{true}$ ;
- $x_{true}$ : MC panel hits mean coordinate;
- The bias ranges between [-6,6] cm;
- Similar distributions for all panels;
- Different straws with different bias;
- $m_{yz} = \frac{\Delta y}{\Delta z}$  not accurately reconstructed.



# Results

- (Top): 2D distribution of  $\Delta x$  vs  $x_{true}$ ;
- Different spots → different overlap regions and muon directions;
- (Bottom):  $\Delta x$  profile vs  $x_{true}$ ;
- $x_{track}$  reconstruction systematics  $\pm 4$  cm;
- $m_{yz} = \frac{\Delta y}{\Delta z}$  not accurately reconstructed;
- Vertical station: **opposite  $y - z$  orientated muons do not cancel out**;
- First spots:  $90^\circ$  panels overlap;
- **Increase of data-taking time**;
- **This calibration is expected to become challenging.**



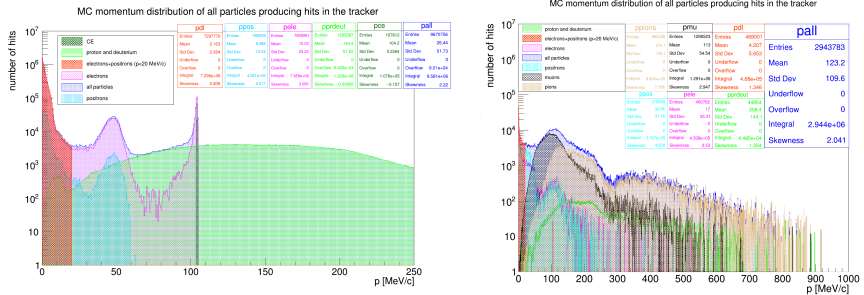
# Outline

- ▶ Commissioning of the tracker DAQ and FEE:
  - validation of ROC readout;
  - study of preamplifiers performance.
- ▶ First steps towards the station calibration;
- ▶ Pre-pattern recognition studies;
- ▶ Conclusions.

# Introduction

- ▶ Most of **tracker hits** are  $e^-$  and  $e^+$  with  $E < 20 \text{ MeV}$  -  **$\delta$ -electrons**:
  - **Compton scattering**: interaction of  $\gamma$ s ( $n$  capture) with material;
  - **$e^\pm$  pairs**: nuclear processes;
  - **$\delta$ -rays**: interaction of high-energy charged particles with material.
- ▶ Mu2e data:  $\geq 7 \text{ PB/year} \rightarrow \text{CPU optimization critical}$ ;
- ▶ Hit flagging is a crucial step for several **physics reasons**:
  - **CE track reconstruction efficiency**;
  - **Protons**: complementary source to determine muon stopping rate;
  - **$\bar{p}$  background**: correct background estimate.
- ▶ **Data-sample** for pre-pattern recognition studies:
  - **CE-1BB**: CE signal + pileup ( $1.6 \times 10^7$  protons/pulse);
  - **CE-2BB**: CE signal + pileup ( $3.9 \times 10^7$  protons/pulse);
  - **PBAR-0BB**:  $\bar{p}$ s and no pileup.

# $\delta$ -electrons in Mu2e tracker

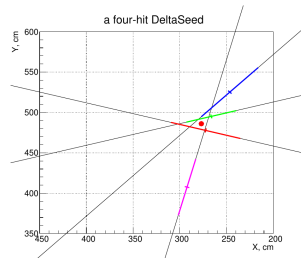
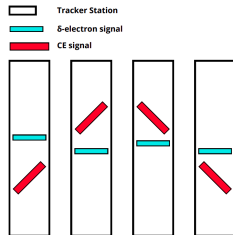


- Momentum distribution of particles making at least one hit in the tracker (Left: **CE-1BB**, Right: **PBAR-0BB**);
- (Left): 75% of hits by  $\delta$ -electrons (71%  $e^-$ , 4%  $e^+$  - Compton scattering);
- (Left): bump in the  $e^+$  distribution ( $N(\mu^+ \rightarrow e^+)/N(\mu^- \rightarrow e^-) \sim 10^{-3}$  for  $\mu$  entering the DS and DIO on IPA should be also  $10^{-3}$  wrt  $\mu^-$  DIF);
- (Right):  $p\bar{p}$  annihilation in ST  $\rightarrow$  multiple tracks with  $p \sim 100/200$  MeV/c.

# $\delta$ -electrons flagging algorithms

Two pre-pattern recognition algorithms developed in Mu2e Offline:

- ▶ **FlagBkgHits (FBH).** First it finds clusters of hits close in  $x - y$  and time and uses an ANN to classify them. Based on *StereoHit* reconstruction. Supervised training with CE+pileup dataset;
- ▶ **DeltaFinder (DF):**
  - $\delta$  segments in each station (*seeds*);
  - straws' center of gravity on  $x-y$ ;
  - *seeds* across stations connected ( $\delta$  candidate);
  - $p$  candidates (*seeds* with  $\bar{E}_{dep} > 3$  keV).



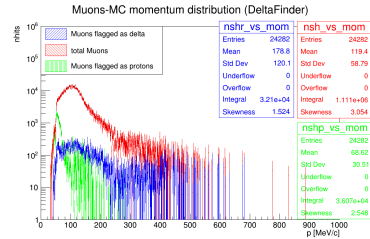
- ▶ (Left)  $\delta$ -electrons and CE in the  $r - z$  plane, (Right)  $\delta$  candidate seed.

# Performance analysis and comparison

Two levels of comparison:

- **hit-level:** how accurately individual hits are flagged (most direct method);
- **high-level:** reconstruction level comparison (figure of merit: CE tracks).
- Before comparing: **proton hit flagging over-efficiency by DF.**

	$f_p$	$f_e$
$p$	96.0%	1.0%
$\mu$	5.8%	5.0%
$\pi$	2.5%	11.2%



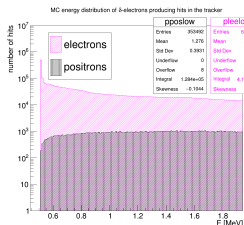
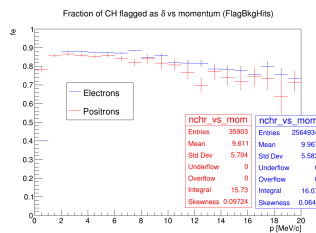
- (Left):  $f_p$  and  $f_e \rightarrow$  fraction of hits flagged as  $p$  and  $e^-$ ;
- (Right): total (red) and flagged (green)  $\mu$  hits vs the particle momentum;
- High  $\mu$  and  $\pi$   $f_p \rightarrow$  low momentum (higher energy deposition as  $p$ );
- *Good* proton candidate  $\rightarrow \geq 4$  hits with  $E_{dep} > 3$  keV;
- $\epsilon_p$  reduced of 10%, but  $\mu$  and  $\pi$   $f_p$  reduced by factor of 2 and 6  $\rightarrow$  next slide.

# Hit-level comparison

- (Top Tab): **PBAR.**  $\mu$  and  $\pi$   
 $f_{p,FBH}$  4x and 3.3x higher;
- $\pi$ : higher momenta;
- (Bottom Tab): **CE-1BB.**  
 Same results for **CE-2BB** within 1%;
- **70% more CE hits flagged** as  $\delta$ s by FBH wrt DF;
- **No  $p$  flagging comparison**  
 (FBH identifies only high  $E_{dep}$  particles);
- (Left):  $e^-$  and  $e^+$   $f_e$  vs momentum (FBH);
- 1-2 MeV: Compton;
- $>2$  MeV: larger  $xy$  spread;
- (Right):  $e^-$  (pink) and  $e^+$  (black)  $E$  distribution  
 $(E < 2$  MeV).

	$f_p$ DF	$f_e$ FBH	$f_e$ DF
$\mu$	2.7%	13.0%	3.2%
$\pi$	0.4%	23.8%	7.3%

	$f_p$ DF	$f_e$ FBH	$f_e$ DF
$e^- < 20$ MeV/c	2.5%	75.9%	72.5%
$e^- [20,80]$ MeV/c	1.0%	50.0%	27.4%
$e^- [80,110]$ MeV/c	0.3%	5.7%	3.4%
$p$	83.7%		1.0%
$e^+ < 20$ MeV/c	0.2%	85.5%	88.5%

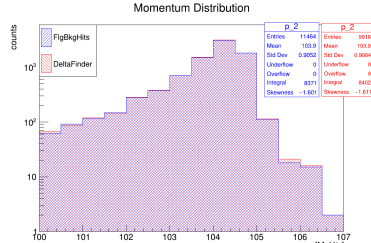
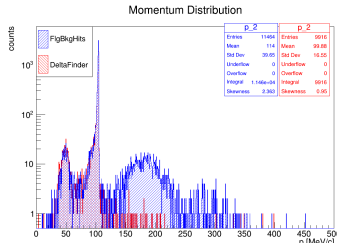


# High-level comparison

- (Top Tab): **PBAR**. DF has 22% advantage in reconstructing 2 tracks (hit-level);
- 80 MeV/c cut: minimum reconstructable particle  $p$  from ST in the tracker;
- 90 MeV/c cut: DIO suppression;
- (Bottom Tab): **CE-1BB**. Same CE reconstruction efficiency (the hit-level difference is 1 hit/track);
- FBH (blue) & DF (red) reconstructed tracks  $p$  distributions (two ranges);
- FBH flags less proton hits and these hits are sent to pattern recognition.

fraction of events	FBH	DF
$N_{tracks} \geq 2$	1.8%	2.2%
$N_{tracks} \geq 2 \text{ & } p > 80 \text{ MeV/c}$	1.7%	2.1%
$N_{tracks} \geq 2 \text{ & } p > 90 \text{ MeV/c}$	1.6%	2.0%

	FBH	DF
CE events with $N_{tracks} > 0$	37.9%	37.9%



# Outline

- ▶ Commissioning of the tracker DAQ and FEE:
  - validation of ROC readout;
  - study of preamplifiers performance.
- ▶ First steps towards the station calibration;
- ▶ Pre-pattern recognition studies;
- ▶ Conclusions.

# Conclusions

- ▶ CLFV processes provide a clean test field for NP models;
- ▶ Mu2e is one of the leading experiments and searches for  $\mu^- N \rightarrow e^- N$ ;
- ▶ Tracker performance is crucial;
- ▶ Comprehensive study from the tracker readout to offline analysis:
  - DAQ and FEE testing:
    - ▶ ROC readout validation with MC at a level of  $10^{-3}$ ;
    - ▶ Preamps: dead channels, cross-talk, and waveform patterns study.
  - First steps towards timing calibration:
    - ▶ Vertical station orientation → non-uniform panel illumination;
    - ▶ Large bias on  $x_{track}$  reconstruction ( $\pm 4$  cm) → data-taking time.
  - Pre-pattern recognition study to flag  $\delta$ -electrons:
    - ▶ Hit-level: FBH flags 70% more CE hits, same performance for  $\delta$ s, no possible  $p$  flag comparison, FBH not trained on  $\bar{p}$  data sample;
    - ▶ High-level: same reconstruction performance for CE signal;
    - ▶ Timing: 0.13, 0.39 ms/ev (1BB, 2BB) more for DF vs 5 ms/ev expected.

**Thank you for your attention!**

# Bibliography

- [1] BERNSTEIN, R.H. AND COOPER, PETER S., *Charged lepton flavor violation: An experimenter's guide*, Physics Reports, 532 (2013), pp. 27–64.
- [2] BERNSTEIN, ROBERT H., *The Mu2e Experiment*, Frontiers in Physics, 7 (2019).
- [3] M. COLLABORATION, *Mu2e Run I Sensitivity Projections for the Neutrinoless  $\mu^- \rightarrow e^-$  Conversion Search in Aluminum*, Universe, 9 (2023).
- [4] H. KOLANOSKI, N. WERMES, *Particle detectors*, Oxford University Press, 2020.
- [5] KARGIANTOULAKIS, MANOLIS, *A search for charged lepton flavor violation in the Mu2e experiment*, Modern Physics Letters A, 35 (2020), p. 2030007.
- [6] L. CABIBBI, G. SIGNORELLI, *Charged Lepton Flavour Violation: An Experimental and Theoretical Introduction*, La Rivista del Nuovo Cimento, 41 (2018), pp. 71–174.
- [7] MU2E COLLABORATION, *Mu2e Technical Design Report*, 2015.

# BACKUP SLIDES

# Beyond the SM

## ► Supersymmetry:

- particle with superpartner (different spin), lepton  $\rightarrow$  slepton;
- no common mass eigenstate base  $\rightarrow$  slepton superposition of flavours;
- CLFV suppression mitigated by  $\nu$  and  $W$  superpartners;
- SUSY breaking at electroweak scale ( $\sim 10^2$  GeV)  $\rightarrow$  observable violation.

## ► Two Higgs Doublet model:

- two Higgs bosons each interacting with fermions;
- non-zero-off-diagonal terms  $\rightarrow$  flavour violating Yukawa couplings.

## ► Leptoquark models:

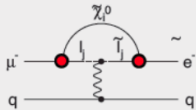
- LQ has both a baryon and lepton number;
- quark and lepton sectors are unified  $\rightarrow$  direct coupling via LQ exchange;
- specific CLFV processes are mediated by LQs.

## ► Additional Neutral Gauge Boson:

- lower energies: gauge groups break down to the direct product of the SM Gauge group  $SU(3) \times SU(2) \times U(1)$  along with an additional  $U(1)$  factor;
- neutral gauge boson mixes with SM neutral Gauge boson;
- two mass eigenstates ( $Z$ ,  $Z'$ );
- off-diagonal terms in neutral current couplings to fermions can lead to flavour-changing couplings to  $Z$  and  $Z'$ .

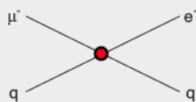
## Supersymmetry

rate  $\sim 10^{-15}$



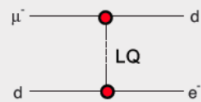
## Compositeness

$\Lambda_c \sim 3000$  TeV



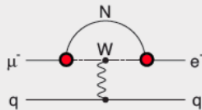
## Leptoquark

$$M_{LQ} = 3000 (\lambda_{\mu d} \lambda_{e d})^{1/2} \text{TeV}/c^2$$



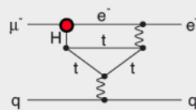
## Heavy Neutrinos

$$|U_{\mu N} U_{e N}|^2 \sim 8 \times 10^{-13}$$



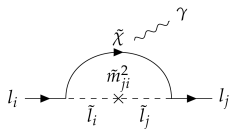
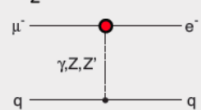
## Second Higgs Doublet

$$g(H_{\mu e}) \sim 10^{-4} g(H_{\mu \mu})$$



## Heavy Z' Anomalous Z Coupling

$$M_{Z'} = 3000 \text{ TeV}/c^2$$



SUSY contribution to  $l_i \rightarrow l_j \gamma$  via slepton

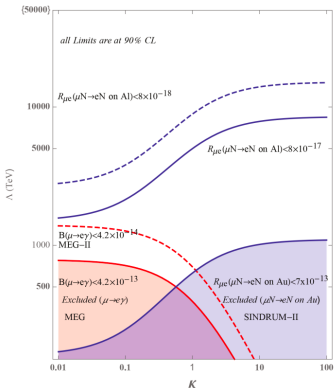
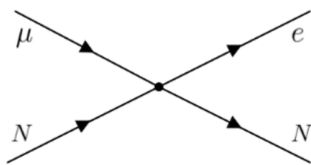
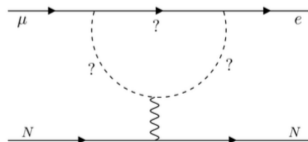
# Muon channels

- ▶  $\mu$  production favored in  $\pi$  and  $K$  decays by hadronic interactions;
- ▶ Long lifetime  $\rightarrow$  muon beams;
- ▶ Small mass: limited number of decay modes available;
- ▶  $\mu^+ \rightarrow e^+ \gamma$ :
  - $e^-$  and  $\gamma$  (52.8 MeV back-to-back);
  - $\mu^+ \rightarrow$  no nuclear capture;
  - Radiative Muon Decay  $\mu^+ \rightarrow e^+ \nu_e \bar{\nu}_\mu \gamma$ ;
  - Accidental Coincidence of  $\mu^+ \rightarrow e^+ \nu_e \bar{\nu}_\mu$  with a  $\gamma$ ;
  - Continuous beam.
- ▶  $\mu^+ \rightarrow e^+ e^- e^+$ :
  - 2  $e^+$  and 1  $e^-$  with total energy equal to the  $M_\mu$ ;
  - Momentum range from few MeV to  $M_\mu/2 \rightarrow$  tracker resolution;
  - Radiative Muon Decay  $\mu^+ \rightarrow e^+ \nu_e \bar{\nu}_\mu \gamma$  with internal conversion;
  - Coincidence of one Michel decay with  $e^+ e^-$  pair (1-MD) or two Michel decays with  $e^+$  (2-MD);
  - Continuous beam.

# Muon channels

- **EFT** Lagrangian parametrisation (model-independent):  $\Lambda$  is the effective mass scale and  $\kappa$  controls the relative contribution of the dipole moment term and the contact term.

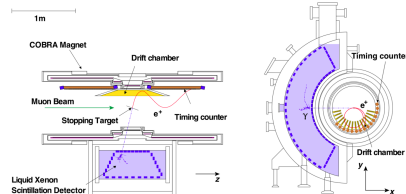
$$\mathcal{L}_{CLFV} = \frac{m_\mu}{(1+\kappa)\Lambda^2} \bar{\mu}_R \sigma_{\mu\nu} e_L F^{\mu\nu} + \frac{\kappa}{(1+\kappa)\Lambda^2} \bar{\mu}_L \gamma_\mu e_L \left( \sum_{q=u,d} \bar{q}_L \gamma^\mu \bar{q}_L \right)$$



# $\mu^+ \rightarrow e^+ \gamma$ experiments

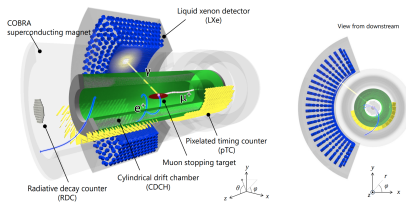
## ► MEG:

- polyethylene target to stop  $\mu$ s;
- anti-bottle  $B$  decreases uniformly from centre, pushing particles away;
- low energy  $e^+$  discarded  $\rightarrow$  detector far from magnet axis;
- drift chamber and timing counters to measure the  $p_{e^+}$  and timing;
- LXe detector for  $E_e$  and  $E_\gamma$ .



## ► MEG II:

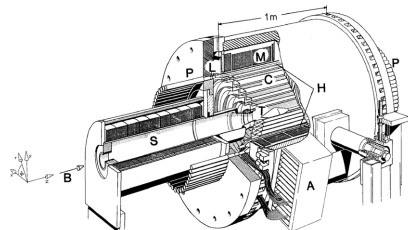
- to reduce the accidental background;
- muon flux increased ( $7 \times 10^7 \mu^+/s$ );
- thinner but more inclined ST;
- new cylindrical drift chamber (higher granularity and transparency);
- pixellated-TC;
- Radiative Decay Counter (low angle  $e^+$ ).



# $\mu^+ \rightarrow e^+e^-e^+$ experiments

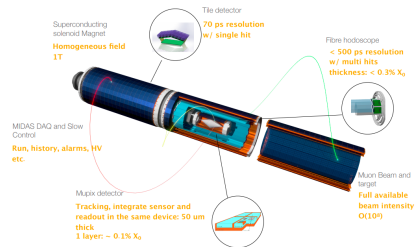
## ► SINDRUM I:

- double cone stopping target in the middle of five concentric multi-wire proportional chambers surrounded by plastic scintillator counters;
- solenoidal magnetic field;
- momentum resolution at the level of  $\sim 1$  MeV, timing resolution  $\leq 1$  ns and a vertex resolution of  $\sim 1$  cm.



## ► Mu3e:

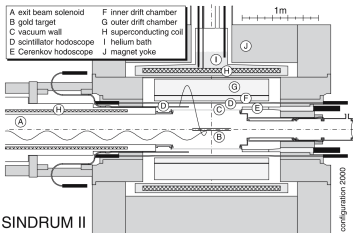
- goal of SES  $\sim 10^{-16}$ ;
- muons stopped on a thin hollow double-cone Mylar target;
- 2 m cylinder detector placed inside a 1.5 T magnetic field in 5 sections;
- pixel detectors and scintillating fiber.



# $\mu^- N \rightarrow e^- N$ experiments

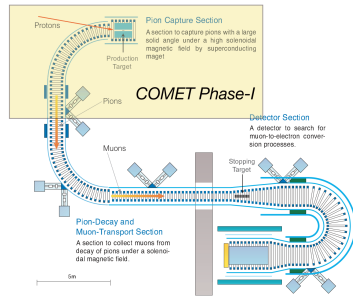
## ► SINDRUM II:

- cylindrical structure;
- target in the middle of the detector;
- 2 drift chambers ( $\text{CO}_2\text{-C}_4\text{H}_1\text{O}$  and  $\text{He-C}_4\text{H}_1\text{O}$ );
- plastic scintillators and Cherenkov for timing and triggering;
- stopped  $\mu$ : Ge(Li) detector.



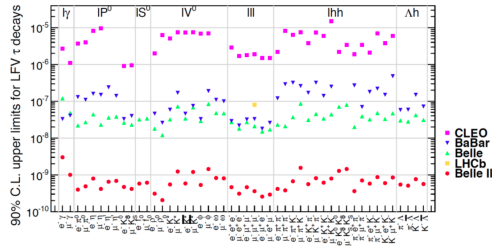
## ► COMET:

- C-shaped transport solenoid: tighter muon momentum selection, with a reduced beam intensity ( $\sim 30\%$  less);
- additional curved solenoid after the stopping target (to remove  $e^-$ );
- Phase-I: understand experimental techniques and backgrounds;
- Phase-II: straw tube tracker and a LYSO EM calorimeter. Magnetic system expanded.



# Tau channel

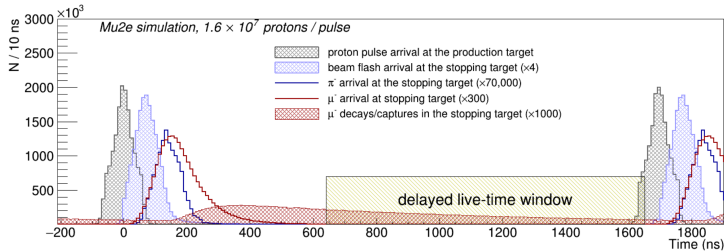
- $\tau$ : promising source of CLFV decays;
- Large mass ( $m_\tau \sim 1.777$  GeV)  $\rightarrow$  multiple CLFV channels;
- $\tau \rightarrow l\gamma$  (radiative decay),  $\tau \rightarrow 3l$  (three-body decay) and  $\tau \rightarrow l h$ ;
- No beams  $\rightarrow \tau_\tau \sim 2.9 \times 10^{-13}$  s;
- Large detectors with good PID, tracking, calorimetry, hermeticity required;
- $\tau^+\tau^-$  produced by  $\Upsilon(4s)$  resonance at  $\sqrt{s} = 10.58$  GeV;
- Wide-range calibrations for detectors.



Reaction	Present limit	CL	Experiment	Year
$\mu^+ \rightarrow e^+ \gamma$	$7.5 \times 10^{-13}$	90%	MEG II	2024
$\mu^+ \rightarrow e^+ e^+ e^-$	$1.0 \times 10^{-12}$	90%	SINDRUM	1988
$\mu^- \text{ Ti} \rightarrow e^- \text{ Ti}$	$6.1 \times 10^{-13}$	90%	SINDRUM II	1998
$\mu^- \text{ Au} \rightarrow e^- \text{ Au}$	$7.0 \times 10^{-13}$	90%	SINDRUM II	2006
$\mu^+ e^- \rightarrow \mu^- e^+$	$8.3 \times 10^{-11}$	90%	SINDRUM	1999
$\tau \rightarrow e \gamma$	$3.3 \times 10^{-8}$	90%	BaBar	2010
$\tau \rightarrow \mu \gamma$	$4.4 \times 10^{-8}$	90%	BaBar	2010
$\tau \rightarrow e e e$	$2.7 \times 10^{-8}$	90%	Belle	2010
$\tau \rightarrow \mu \mu \mu$	$2.1 \times 10^{-8}$	90%	Belle	2010

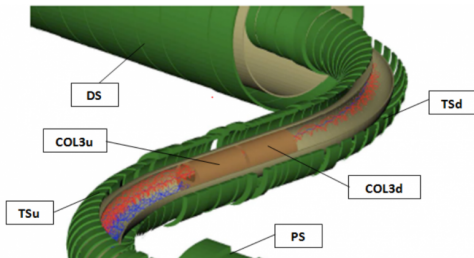
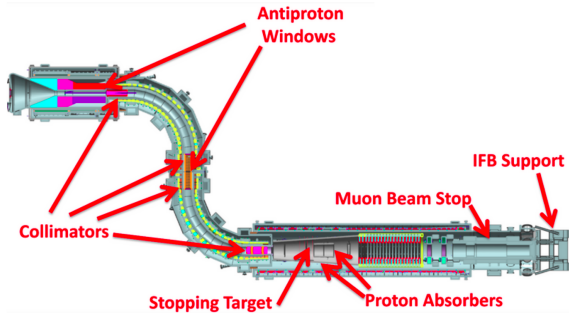
Table: Experimental upper limits for CLFV processes (leptons).

# Pulsed proton beam



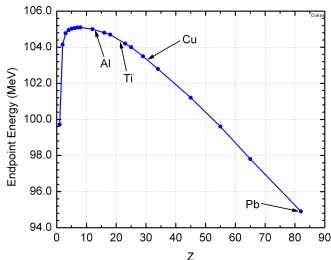
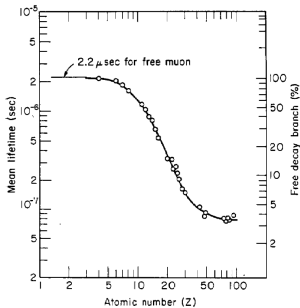
- ▶ 8 GeV, 8 kW beam originates from the Fermilab Booster;
- ▶ Proton pulses separated by 1695 ns and the delayed window is after 640 ns after the first pulse;
- ▶ Due to the short lifetime of pions, this background can be suppressed by using pulsed proton beam along with a delayed live-time window.

# Mu2e beamline



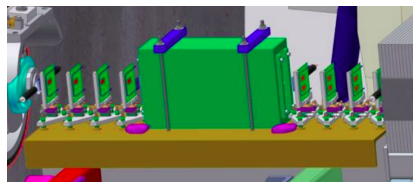
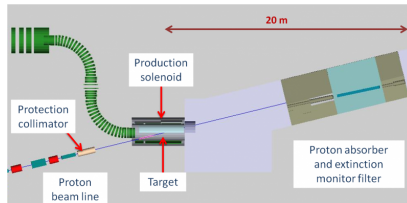
# Why Al Stopping Target?

- ▶ Lower RMC background. Photon endpoint:  $k_{max} = m_\mu c^2 - |E_b| - E_{rec} - \Delta M$   $\sim 101.9$  MeV;
- ▶ Long lifetime: better separation between prompt backgrounds and live window;
- ▶ High Al DIO endpoint: Higher- $Z$  nuclei  $\rightarrow$  lower endpoint, minimizing background contribution;
- ▶ Conversion  $BR$  depends on the ST material. Materials with higher  $Z \rightarrow$  better model differentiation (Mu2e-II: Ti);
- ▶ Available in required size/shape/thickness, low costs and chemically stable.



# Extinction monitor

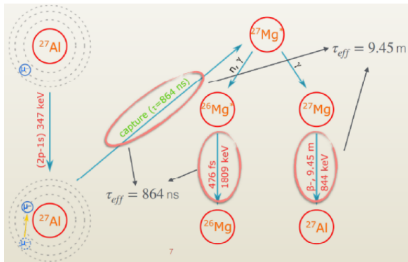
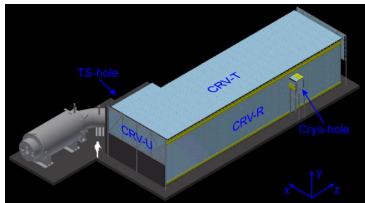
- ▶ Mu2e requirement: extinction  $< 10^{-10}$ ;
- ▶ Two factors contribute to extinction:
  - intrinsic accelerator extinction ( $2.1 \times 10^{-5}$ );
  - Mu2e AC dipoles sweep away out-of-time protons into collimators ( $5 \times 10^{-8}$ ).
- ▶ Extinction Monitor (EM): collimator and magnetic filter system, pixel telescope;
- ▶ EM measures out-of-time protons;
- ▶ Magnetic filter transport of particles generated at the PT to the EM;
- ▶ The pixel telescope tracks the trajectory and momentum of particles (permanent magnet + 8 scintillators).



# Cosmic Ray Veto and Stopping Target Monitor

## Cosmic Ray Veto:

- ▶ **Active veto:** 4 layers of extruded plastic scintillation counters;
- ▶ **Passive shielding:** Al absorbers between each layer;
- ▶  $\epsilon_{CRV} = 99.9\%$ ;
- ▶  $\mu$ 's signature: 3/4 vetoed.

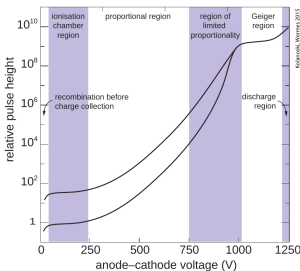
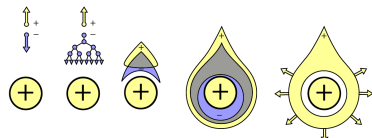
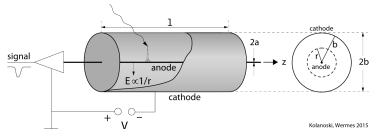


## Stopping Target Monitor:

- ▶ HPGe and LaBr<sub>3</sub> detector → number of  $\mu$  stopped in ST (10% precision on  $N_\mu$ );
- ▶ It will measure the photons produced by secondary muonic aluminium orbital transitions (347 keV) and nuclear capture (884 keV, 1809 keV);
- ▶ Captured  $\mu = 61\%$  of stopped  $\mu$ .

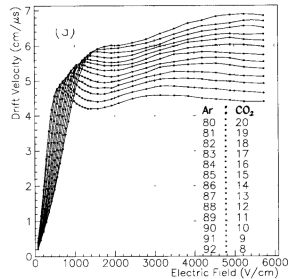
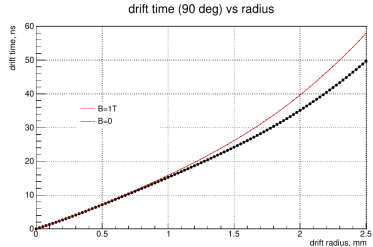
# Drift tubes

- ▶ Cathode: grounded cylindrical conductor;
- ▶ Anode wire → high voltage  $\mathcal{O}(\text{kV})$ ;
- ▶ Gases combination: noble ( $A$ ) + quench gas ( $B$ );
- ▶  $E(r) = \frac{1}{r} \frac{\lambda}{2\pi\epsilon} = \frac{1}{r} \frac{V}{\ln(b/a)}$  ( $a < r < b$ );
- ▶ Primary ionisation:  $A C \rightarrow A^+ e^- C$ , or  $A C \rightarrow A^{++} e^- e^- C$ ;
- ▶ Excitation:  $A C \rightarrow A^* C \rightarrow A^* B \rightarrow AB^+ e^-$  or  $A^* A \rightarrow A_2^+ e^-$ ;
- ▶ Secondary ionisation → avalanche;
- ▶ Proportional region;
- ▶ Quench gas ( $\text{CO}_2$ ) absorbs  $\gamma$ s from recombination preventing subsequent avalanches.



# Drift tubes in magnetic field

- Electric drift and magnetic field:
  - drift direction and velocity change ( $B \uparrow \rightarrow v_d \downarrow$ );
  - reduction of diffusion transverse to the magnetic field.
- Type of drift gas and magnetic-electric field relative orientation;
- $\vec{v}_D^B = -\frac{\mu^{B=0}}{1+\omega^2\tau^2} \left( \vec{E} + \frac{\vec{E} \times \vec{B}}{B} \omega \tau + \frac{(\vec{E} \cdot \vec{B}) \vec{B}}{B^2} \omega^2 \tau^2 \right)$ ;
- $\mu_B = 0$ : mobility with  $B = 0$ ;
- $\omega = \frac{qB}{m}$ : cyclotron frequency;
- $\tau$ : average collision time in the gas;
- Straws  $\perp$  to  $B$ ;
- $\alpha_{v_d B} \in (0^\circ, 90^\circ)$ ;
- Ar:CO<sub>2</sub>:  $v_d$  depends on the electric field;
- 8 ns at a radial distance of 2.5 mm.

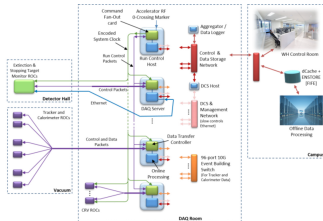


# Tracker data format

A **hit data packet** has a fixed length of 32 bytes:

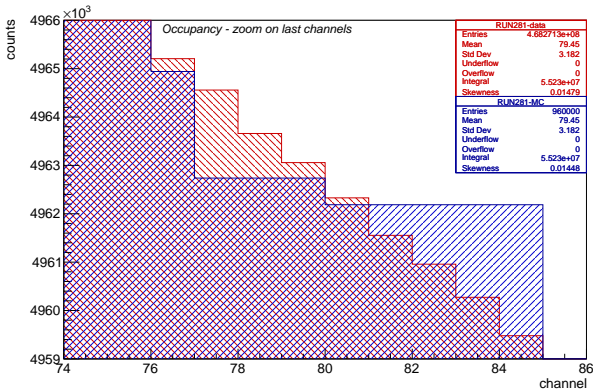
- ▶ 16 bit header (straw index);
- ▶ 16 bit for the TDC left straw end;
- ▶ 16 bit for the TDC right straw end;
- ▶ 8 bits for the ToT (time-over-threshold) for the two ends;
- ▶ 12 bits for each ADC samples. For each hit, a fixed number of samples (15) is readout;
- ▶ 12 bits are set aside for preprocessing flags.

# DAQ system



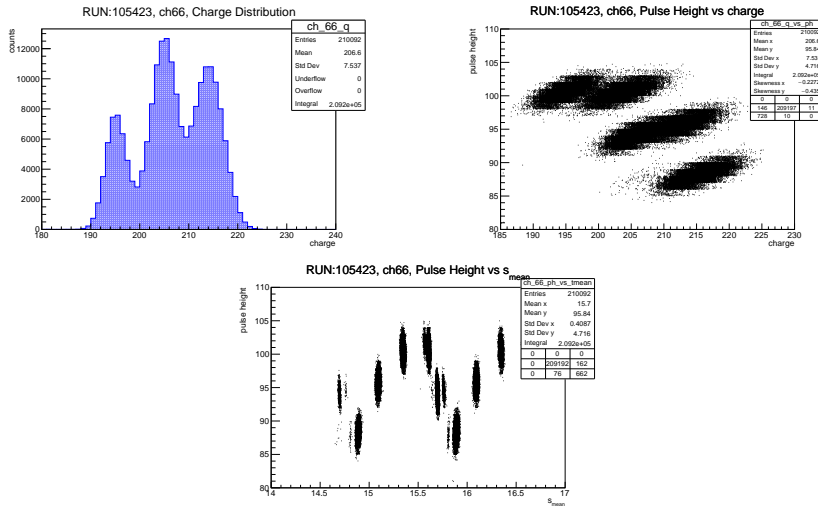
- ▶ *Streaming readout:* digitized and zero-suppressed data, flexible for analysis;
- ▶ DAQ run control via RCH, managing a predefined Run Plan;
- ▶ Active spill defined by proton pulses, defining the EW;
- ▶ CFO module generates 40 MHz clock, embedding EWMs;
- ▶ CFO distributes the clock and run control packets to DTCs in DAQ servers;
- ▶ DTCs pass the clock to ROCs and EWMs are recovered;
- ▶ ROCs use EWMs to separate data from consecutive EWs;
- ▶ Data Requests trigger ROC data transmission through DTCs;
- ▶ EBS routes data from multiple DTCs for online analysis;
- ▶ Events logged and transferred to long-term storage ( $\geq 7$  PB/year);
- ▶ DTCs handle slow control data, managed by DCS Host and stored.

# Additional plots



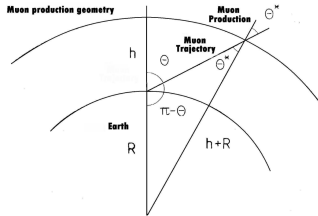
- ▶ Zoom on the last readout channels of the occupancy plot.

# Additional plots



- ▶ (Left): The (positive) charge distribution of the waveforms (channel 66);
- ▶ (Right): 2D distribution of pulse height versus (positive) charge.

# Cosmic muons simulation with CRY



- ▶ CRY (LANL) was used to generate cosmics (straightforward implementation);
- ▶ It simulates protons (1 GeV, 100 TeV), at the top of the atmosphere and generation of muons from the pion decays.
- ▶ It follows Gaisser-Tang model:

$$\frac{dI}{dE_\mu d\Omega dt dS} = \frac{0.14}{\text{cm}^2 \text{ s sr}} \left( \frac{E_\mu}{\text{GeV}} \left( 1 + \frac{3.64 \text{ GeV}}{E_\mu (\cos \theta^*)^{1.29}} \right) \right)^{-2.7} \left[ \frac{1}{1 + \frac{1.1 E_\mu \cos \theta^*}{115 \text{ GeV}}} + \frac{0.054}{1 + \frac{1.1 E_\mu \cos \theta^*}{850 \text{ GeV}}} \right];$$

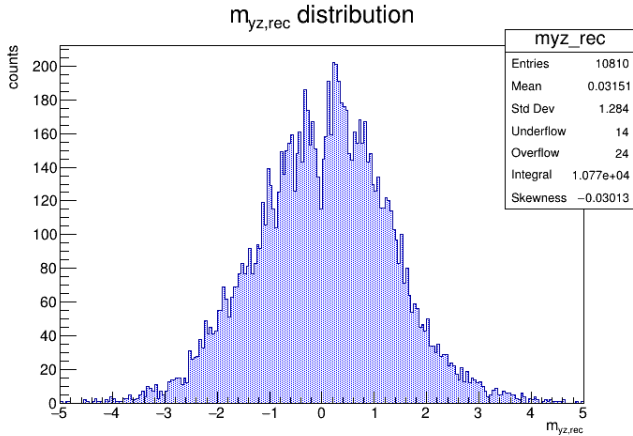
- ▶  $\cos \theta^*$  is given by:  $\cos \theta^* = \sqrt{\frac{(\cos \theta)^2 + P_1^2 + P_2(\cos \theta)P_3 + P_4(\cos \theta)P_5}{1 + P_1^2 + P_2 + P_4}}$  with  $P_1 \sim 0.10$ ,  $P_2 \sim -0.07$ ,  $P_3 \sim 0.96$ ,  $P_4 \sim 0.04$  and  $P_5 \sim 0.82$ ;
- ▶ (Top):  $\theta^*$  and  $\theta$ , zenith angle of muons and at the muon production point.

# How to determine channel-to-channel delays

$$\frac{(t_1 + t_2)}{2} = t_d + t_0 + \frac{d_1 + d_2}{2} - \frac{L}{2v}$$

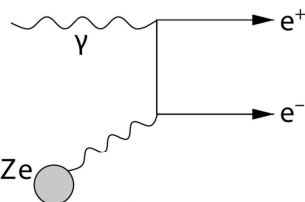
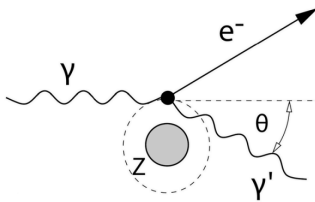
- ▶  $(t_1 + t_2)/2$  allows to measure the drift time up to an offset common to all channels.

# Reconstructed muon direction



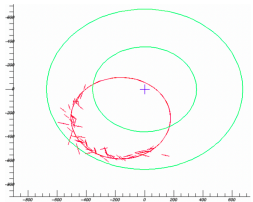
- ▶ Lots of muons reconstructed with  $m_{yz} \sim 0$  (horizontal);
- ▶ The true hit position, far from the straws midpoint, results in incorrectly reconstructed tracks' direction on the  $y - z$  plane.

# $\delta$ -electron sources

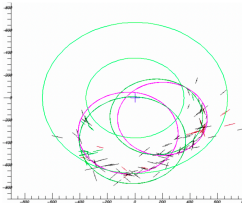


- **Compton scattering:** scattering of a  $\gamma$  by a free or quasi-free ( $E_\gamma \gg E_B$ ) electron of detector material.  
Muon capture  $\rightarrow$  neutrons  $\rightarrow$  neutron capture  $\rightarrow \gamma$  emission ( $E_\gamma \sim \text{MeV}$ ).  
 $e^-/e^+$  asymmetry. Compton cross section per atom proportional to  $Z$ ;
- **Pair production:** from nuclear processes. In the Coulomb field of a charge, a photon can convert into an  $e^- - e^+$  pair.  $Z^2$  dependence.  
$$E_\gamma \geq 2m_e c^2 + 2\frac{m_e^2}{m_{\text{nucleus}}}c^2;$$
- **Delta rays** (or secondary ionization electrons): generated when high-energy charged particles collide with the detector material.  
A particle collides with shell  $e^-$ , resulting in significant energy transfers.

# $\bar{p}$ background in Mu2e



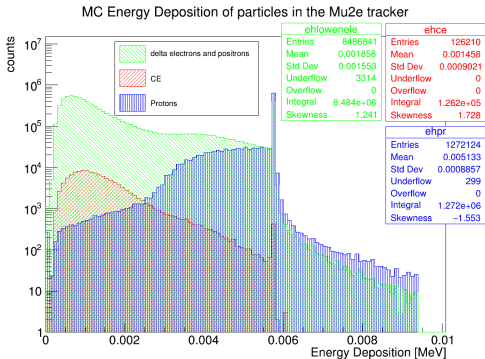
XY view



XY view

- ▶  $\bar{p}s$  are produced from  $pW$  interactions;
- ▶  $p\bar{p}$  annihilation at ST  $\rightarrow e^-$  by  $\pi^0 \rightarrow \gamma\gamma$  followed by  $\gamma$  conversions and  $\pi^- \rightarrow \mu^- \bar{\nu}$ ;
- ▶ The background cannot be suppressed by cuts on the time window because  $\bar{p}s$  are slower than other beam particles;
- ▶ There are absorber elements placed in the TS to suppress the  $\bar{p}s$ ;
- ▶  $p\bar{p}$  annihilation at ST can give multiple particle tracks with  $p \sim 100$  MeV/c for each track at much higher rate than signal-like;
- ▶ From MC, it was estimated that the rate of such multi-track events is  $\times 500$  higher than the rate of events with 1 signal like  $e^-$ ;
- ▶ The analysis aims to reconstruct the multi-track final state events and get an estimate of the CE like events by rescaling the two final states ratio.

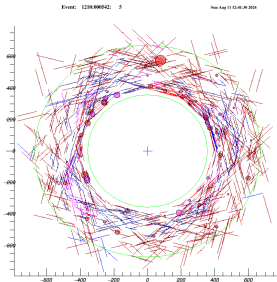
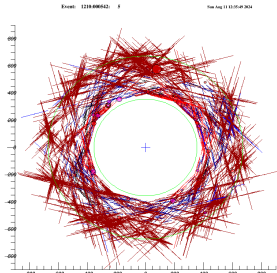
# Monte Carlo deposited energy in the tracker



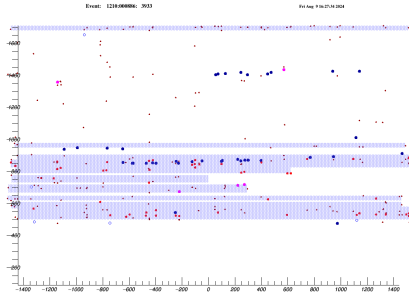
- The Monte Carlo deposited energy distribution in the tracker (*CE – 1BB data sample*);
- (Red) CEs, (green)  $\delta$ -electrons, (blue) protons.
- Peaks and tails → saturated waveform;
- Only about 4% of CE hits have energies above 3.5 keV (1% above 5 keV);
- Applying an energy threshold in DF can speed up processing, but impacts algorithm efficiency, especially in *seed* reconstruction.

# Mu2e event reconstruction

- ▶ Mu2e event reconstruction is optimised to reconstruct single-track events with tracks coming from the ST;
- ▶ Adjacent *StrawHits* within a panel, which are most likely due to the same particle, are combined into a *ComboHit*;
- ▶  $\delta$ -electron pre pattern recognition;
- ▶ We cluster the hits within a time window to form *TimeClusters* assuming that such hits are made by the same particle;
- ▶ Hits from *TimeClusters* are used to form helices;
- ▶ Final parameters of the track are determined by the Kalman fit.



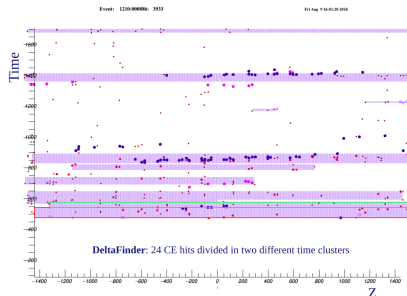
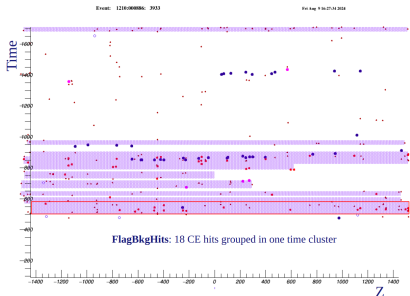
# Time Clustering



## Time clustering process:

- ① Combination of at least 3 *ComboHits* within a specific  $time - z$  window (with a 20 ns time window and a 5-plane z-window);
- ② *Chunks* are created;
- ③ Every potential pair of chunks within a certain time proximity is tested together, and the pair, that minimizes the  $\chi^2/ndof$  when the hits are fit to a linear line, is combined;
- ④ Procedure repeated until no further combinations yield a  $\chi^2/ndof$  below a set threshold.

# Time Clustering development



- ▶ There is a well defined class of events where the effects of hit flaggers get washed out in the reconstruction by the time clustering algorithm;
- ▶ Example:
  - DF: hits from one particle divided in two different time clusters;
  - FBH: not flagged particle hits are used by the time clusterer to *connect* particle hits that are used in the reconstruction. That is why the track is reconstructed in this case.
- ▶ Improving the cluster finder and the pattern recognition could increase the track reconstruction performance.